Reconstructing antibody dynamics to estimate the risk of influenza virus infection

Tim Tsang
University of Hong Kong
Ranawaka Perera
The Univeristy of Hong Kong
Vicky Fang
The University of Hong Kong
Jessica Wong
The University of Hong Kong
Eunice Shiu
University of Hong Kong
Hau Chi So
University of Hong Kong
Dennis Ip
The University of Hong Kong
Malik Peiris
University of Hong Kong https://orcid.org/0000-0001-8217-5995
Gabriel Leung
School of Public Health, LKS Faculty of Medicine, The University of Hong Kong https://orcid.org/0000-0002-2503-6283
Benjamin Cowling (bcowling@hku.hk)
University of Hong Kong https://orcid.org/0000-0002-6297-7154
Simon Cauchemez
Institut Pasteur

Article

Keywords: influenza virus infections, antibody titers, individual infection risk

Posted Date: October 26th, 2021

DOI: https://doi.org/10.21203/rs.3.rs-998475/v1

Version of Record: A version of this preprint was published at Nature Communications on March 23rd, 2022. See the published version at https://doi.org/10.1038/s41467-022-29310-8.

Abstract

For >70 years, a 4-fold or greater rise in antibody titer has been used to confirm influenza virus infections in paired sera, despite recognition that this heuristic can lack sensitivity. Here we analyze with a novel Bayesian model a large cohort of 2,353 individuals followed for up to 5 years in Hong Kong to characterize influenza antibody dynamics and develop an algorithm to improve the identification of influenza virus infections. After infection, we estimate that hemagglutination-inhibiting (HAI) titers were boosted by 16-fold on average and subsequently decrease by 14% per year. Greater boosting in HAI titer is observed in epidemics with a circulating strain that is different from the previous epidemic. In six epidemics, the infection risks for adults were 3%-19% while the infection risks for children were 1.6-4.4 times higher than that of younger adults. Every two-fold increase in pre-epidemic HAI titer was associated with 19%-58% protection against infection. Among the 1731 infections inferred by our model, around half were missed by the 4-fold rise criteria, suggesting that this criteria underestimates infection risks by 23-70%. The sensitivity and specificity of identifying infections for our approach are 87% (95% CrI: 85%, 89%) and 98% (95% CrI: 97%, 98%) respectively, which are higher than 82% (95% CrI: 80%, 84%) and 96% (95% CrI: 96%, 97%) for using 4-fold rise criteria. Our inferential framework clarifies the contributions of age and pre-epidemic HAI titers to characterize individual infection risk and offers an improved algorithm to identify influenza virus infections.

Introduction

Each year, influenza virus causes an estimated three to five million severe illnesses and 400,000 deaths on average [1]. In addition, avian influenza viruses can occasionally adapt to humans and cause influenza pandemics. A thorough characterization of the risk factors for influenza virus infection is critical to optimize mitigation strategies, and an important component of this is correct identification of infected persons. However, it can be challenging to determine whether a person has experienced an influenza virus infection, since most infections are associated with mild disease or are asymptomatic [2–4]. Serological studies can allow identification of infections regardless of illness severity, and can be used to estimate the incidence of influenza virus infections in different regions and in persons of different ages [2, 5–8].

For more than 70 years, scientists have relied on an ad-hoc rule whereby a 4-fold or greater rise in hemagglutination-inhibiting (HAI) titers in paired sera is considered as evidence of influenza virus infection [9, 10]. Although this can capture some asymptomatic and subclinical infections, there are a number of known limitations to this heuristic, such as misclassification due to measurement error [11], and ‘non-bracketing’ issue that the first serum is collected after infection [12]. Consequently it can be difficult to estimate infection rates in communities [11, 12], and characterize disease severity [13], disease burden [1, 14] and risk factors for infection [15] since all of these require accurate classification of infected vs uninfected persons.

Here, we develop an analytical framework to address this challenge. We develop a novel Bayesian model to characterize the dynamics of influenza HAI titers from the analysis of a large cohort of 2,353 individuals followed for up to 5 years in Hong Kong. Using this detailed understanding of HAI dynamics, we build an algorithm that can identify influenza infections without having to rely on fixed and arbitrary cut-offs. We use our approach to build a comprehensive picture of the circulation of influenza in Hong Kong and its footprint on HAI titers in the population. We then use the model to perform joint estimation of infection risks in different age groups during six influenza epidemics in Hong Kong from 2009 through to 2013, the risk factors for infection, the degree of boosting and waning in HAI titer after infection, and the measurement errors in HAI titer.

Results

Study participants and influenza epidemics

A total of 3,160 individuals participated in the studies in 2008/09 or 2009/10 including 301 who participated in both studies [16, 17]. Participants were then followed up for three additional years with an average annual drop-out rate of 15% [18]. Based on the surveillance data, there were three epidemics of influenza A(H1N1)pdm09 and three seasonal influenza A(H3N2) epidemics (hereafter abbreviated as H1N1 and H3N2 respectively) in the study period (Figure 1A). Among each of the the 6 epidemics, there are between 1321 and 1851 individuals with at least one mid-/post-epidemic HAI titers among individuals and included in the analysis (Figure S1, Table S1). Figure 1B illustrates titer trajectories for three individuals that are considered uninfected based on the traditional 4-fold rise approach.

HAI titer dynamics

We estimate that, after infection, geometric mean HAI titers are boosted 3.98 (95% CrI: 3.89, 4.07) $\log_2$ titers on average, with standard deviation 1.82 (95% CrI: 1.77, 1.88), and 14% (95% CrI: 12%, 16%) of infections are associated with less than 4-fold rises (Figure 1C). For H1N1, a strain change is associated with a mean boost in adults that was 1.26 $\log_2$ titers (95% CrI: 0.78, 1.73) higher in epidemic 1 (with strain change; Table S3) than in epidemics 3 and 5 (without strain change; Table S3). The effect was similar in children (1.58 $\log_2$ titers; 95% CrI: 1.10, 2.07). For H3N2, the mean boost in epidemic 4 (with strain change; Table S3) was also higher than in epidemics 2/6 (without strain change; Table Sxx): 1.54 $\log_2$ titers (95% CrI: 0.73, 2.39) higher for children and 1.45 $\log_2$ titers (95% CrI: 0.94, 1.96) higher for adults. For H1N1, the mean boosting in children was 0.64 $\log_2$ titers (95% CrI: 0.21, 1.04) and 0.95 $\log_2$ titers (95% CrI: 0.41, 1.50) higher than in adults, in epidemic 1 and epidemic 3/5, respectively. There was no difference in boosting in children and adults for H3N2.

After the boost following infection, the HAI titer starts to wane, with a mean waning rate of 14% (95% CrI: 12%, 15%) a year after infection, and a standard deviation of 22% (95% CrI: 21%, 23%). We also observe substantial differences in the waning rate depending on the epidemic (Figure 1D). For H1N1, we estimate

that the waning in epidemic 1 (with strain change) is 27% (95% CrI: 11%, 40%) and 53% (95% CrI: 27%, 84%) more than in epidemic 3/5 (without strain change) for children and adults respectively. For H3N2, we estimate that the waning in epidemic 4 (with strain change) is 21% (95% CrI: 8%, 40%) larger than in epidemic 2/4 (without strain change) for children, but no difference for adults. Overall, we find that when the circulating strain is substantially different than the previous ones, HAI titers exhibit larger boost and waning than those seen in other years.

We estimate that the 1-sided probability of a 2-fold error is 2.8% (95% CrI: 2.3%, 3.6%) and 5.5% (95% CrI: 4.9%, 6.1%) for H1N1 and H3N2, respectively. The probability that the measurement is erroneous and that observed HAI titer level is a random value from <10 to 5120 is 3.3% (95% CrI: 2.9%, 3.7%).

Our framework allows us to reconstruct the antibody titer dynamics to identify infections probabilistically, integrating information on observed titers, the boosting and waning distribution, measurement error, and influenza activity. For example, our model suggests that the Child 1 in Figure 1B that has a 2-fold rise in epidemic 1 was likely infected with probability 0.81. Due to irregular seasonality in Hong Kong and unpredictable timing of influenza circulation [12, 19–21], the pre-epidemic titer may be missing and infection may have occurred before the collection of the first sample (Figure S1). For example, Adult 1 in Figure 1B has HAI titer equal to 3 in $\log_2$ scale in the first and second sample but we infer that this individual has an 80% chance to have been infected. This is because almost all individuals have an HAI titer <10 before the pandemic while there was also high prevalence of infection in the community during the pandemic (estimates shown in the next section). In contrast, Adult 2 in Figure 1B has the same observed titer pattern in a seasonal epidemic but since the probability of infection in the community is low during this epidemic, it is unlikely this individual was infected (probability of 0.08). These simple examples illustrate the additional insight one can gain from an analysis that goes beyond the 4-fold rise case definition and can integrate additional contextual information.

Using the same technique for each individual, among 9463 person-epidemic investigated over six epidemics, we probabilistically identify 1731 infections (95% credible interval (CrI): 1657, 1791). Among these, 45% of those infections (779; 95% CrI: 736, 807) have no pre-epidemic titers and could therefore not be identified by the traditional 4-fold cutoff point. Among 662 individuals with 2-fold rise in paired sera, we estimate that 24% of those (160; 95% CrI: 139, 192) were infected.

Infection risk in epidemics

We estimate the infection probability for children (age <18), adults (age 18-50) and older adults (age >50) during six epidemics (Figure 2A). For the 2009 H1N1 pandemic, these probabilities were 52% (95% CrI: 48%, 56%), 19% (95% CrI: 16%, 21%) and 13% (95% CrI: 8%, 19%) respectively. During seasonal epidemics 2-6, they were in the range 4%-22% for children, 3%-15% for adults, and 2%-17% for older adults. However, these overall infection probabilities reflect the combination of the effects of age, the distribution of pre-epidemic HAI titers across age groups and the level of protection associated with different HAI titers. First, the infection probability for individuals with a given pre-epidemic titer could vary by epidemic. The infection probabilities during epidemics 5-6 were smaller than for epidemics 1-4 for individuals with pre-

epidemic HAI titer <10, and children were at higher risk than adults even when they both had HAI titers <10 (Figure 2A). Second, the average pre-epidemic titers for children (log_2 titer: 3.1) are higher than adults (log_2 titer: 1.4) among the five seasonal epidemics (Figure 2B). Third, the protection associated with a two-fold increase in pre-epidemic titer (Figure 2C) ranges from 38–58%, except in epidemic 4, where the protection is only 19% (95% CrI: 13%, 28%). Therefore, after adjusting for the higher average pre-epidemic titers of children, their infection probabilities are still estimated to be 1.6 to 4.4 times higher than that of younger adults in the six epidemics (Figure 2D).

Association between infection status in different epidemics

We explore the association between infection status in different epidemics, considering individuals that participated in more than one epidemic in our study (n=1853; Table S2). For adults, there is no evidence for heterosubtypic protection from previous infections (Figure 3 and S2). For children, infection during H1N1 epidemic 1 provides 93% (95% CrI: 83%, 98%) and 76% (95% CrI: 25%, 96%) protection in H1N1 epidemic 3 and 5, respectively. Such homosubtypic protection is not observed for H3N2. However, the association is no longer significant after adjusting for pre-epidemic HAI titers in the logistic regression, suggesting such protection is captured by information on pre-epidemic HAI titers boosted by previous infections.

Sensitivity and specificity of identifying infections

We conducted a simulation study to compare the sensitivity and specificity of identifying infections by using our approach or using a 4-fold cutoff point. We use our model with the model parameters randomly drawn from their posterior distribution to simulate 50 epidemics. When pre-epidemic titers are available, the sensitivity and specificity of our approach are 87% (95% posterior predictive intervals (PPI): 85%, 89%) and 98% (95% PPI: 97%, 98%), which is better than the ones obtained using a 4-fold cutoff point, with 82% (95% PPI: 80%, 84%) sensitivity and 96% (95% PPI: 96%, 97%) specificity. Moreover, our framework performs substantially better when the pre-epidemic titers are unavailable, with 78% (95% PPI: 73%, 81%) sensitivity and 96% (95% PPI: 95%, 97%) specificity compared to the 4-fold rise case definition. Using a 4-fold cutoff point would have only 22% (95% PPI: 20%, 24%) sensitivity and 98% (95% PPI: 98%, 99%) specificity, due to the ‘non-bracketing’ problem that individuals infected before the collection of the first serum samples are misclassified as uninfected [12].

Model validation and adequacy

Based on 50 simulated epidemics, we found that the 4-fold rise case definition leads to an underestimation by 44-70% of infection probabilities for the first three epidemics in which there are non-bracketing issue so that the pre-epidemic titer for some individuals are unavailable (Figure 4A). In addition, the infection probabilities for children are underestimated by 23%-59% for the other three epidemics with no non-bracketing issue. Furthermore, the age relative susceptibility may be biased if using a 4-fold cutoff point to identify infections, particularly for children (Figure 4B).

In a simulation study with 50 epidemics, we validated that our approach can accurately identify infections by computing the proportion of infections in individuals with model-predicted infection probabilities that fell in the infection probability window (10 intervals from 0 to 1). We found that the proportion of infections are equal to the middle value of each probability window, suggesting that our inference can correctly identify infections (Figure 4C). We found that the distributions of titer change predicted by the model for children and adults in each epidemic are consistent with the observed ones (among 1000 simulated epidemics) (Figure S3). In 50 simulated epidemics, we find our approach could adequately estimate model parameters with no systematic bias (Table S4).

Discussion

In this study, we developed a Bayesian modeling approach to jointly estimate individual antibody dynamics, identify influenza virus infections, and determine the risk factors for infection. We found that our approach outperformed the use of the 4-fold rise case definition which may cause under-detection of infections and hence underestimation of infection risks [11, 12]. Compared with previous approaches that used the antibody titer response after PCR-confirmed infections to identify infections without using the traditional 4-fold rise approach [22, 23], our approach jointly characterized antibody titer dynamics to identify infections based on serology data alone and, did not require any PCR-related data. Instead, we used surveillance data to inform estimation of infection time, which would be much easier to obtain and would be much more suitable for serologic studies [6].

We estimated the degree of boosting of HAI titers after H1N1 and H3N2 infections, and their waning after the boost. We estimated that higher boosting occurred in children, and after strain changes in epidemics, which is consistent with the results from previous studies [24, 25]. Both associations are likely caused by the infection histories, as previous exposure to similar strains would reduce the HAI titer response [26–28] and children are less likely to have been previously exposed than adults. We found that the waning in HAI titer was higher in epidemics with strain change for both H1N1 and H3N2. Such higher waning was also observed in other studies [7, 12, 23, 29–31]. Further studies are required as the waning rate could depend on other factors, such as the definition of cases, previous exposure or age [12, 22, 26].

Our findings indicate that there is a complex interaction between age and individual immunity. In our framework that accounted for variability in HAI assays [32], we find that the protection associated with HAI titer could vary by epidemic, similar to other studies [15, 19, 30, 33–35]. Also, we find that the infection probabilities for children and adults could differ after adjusting for HAI titers, which could be because HAI titers only capture part of the immunity for adults [22, 26, 34], or that children have greater exposure to infection for various reasons [33, 36]. Despite these age differences in infection probabilities, we still find that HAI titers predict infection probabilities at the individual level, and the protection from prior infection could be explained by HAI titer that was boosted by previous infections. This suggests that the distribution of HAI titers in a population could be a useful measure of the proportion of individuals with protection, as a measure of population immunity [7].

Our approach consistently outperforms the traditional 4-fold cutoff for both sensitivity and specificity. Therefore, our approach could give a more accurate estimate of the incidence of infections and hence more accurate determination of risk factors and disease burden. In particular, our approach could account for the different boosting and waning patterns and therefore would be generalizable to populations with persons with different boosting and waning distribution for different influenza virus strains or even other pathogens with similar patterns after infections [37]. Furthermore, our approach could still perform well when there is a “non-bracketing” issue that collected sera may not neatly bracket the epidemics of interest. Such performance would be critical as “non-bracketing” is unavoidable in tropical and subtropical regions, or in unpredictable influenza pandemics [20, 38, 39].

Our study has some limitations. We used a proxy measure of influenza activity in the community (Figure 1A) and the reliability of estimates would depend on the accuracy of the proxy to reflect the relative infection risk over time. Although the proxy is not age-specific, our previous study suggested that the incidence rate of H1N1 infection in 2009 pandemic were similar among different age groups [40]. Since the rise in HAI titer from vaccination is indistinguishable from natural infections, we excluded all recently vaccinated individuals in this analysis, and our results may not be generalizable if vaccination has an effect on infection risk over more than one epidemic.

In conclusion, here we introduced a new approach to jointly characterize antibody dynamics and identify influenza virus infections from serological data that addresses key limitations of the tradition 4-fold rise case definition. Within our inferential framework, we were able to clarify the contributions of age and pre-epidemic titers to characterize individual infection risks.

Methods

Study design

Data were collected from two community-based randomized controlled trials (RCTs) for evaluating direct and indirect benefits of influenza vaccination (Appendix Section 1) [16, 17]. In the RCTs conducted in 2008/09 and 2009/10, 119 and 796 households were recruited. Serum specimens were collected at the start of the study, and after 6 and 12 months from all participants. In the subsequent observational follow-up of the same cohort participants from late 2010 to late 2013 without intervention [18], serum specimens were collected from all participants in each autumn (October to December), and also each spring (April to May). Receipt of influenza vaccine outside of the trial was recorded annually.

Laboratory Methods

All serum specimens were tested in parallel for antibody responses by hemagglutination inhibition (HAI) assays in serial doubling dilutions from an initial dilution of 1:10 using standard methods [41]. The reciprocal of the highest dilution of serum that prevents complete hemagglutination wells was regarded as the antibody titer. In the pilot (2008/09), serum specimens were tested against A/California/7/2009(H1N1) and A/Brisbane/10/2007(H3N2). In the main trial and second year of follow-

up, i.e. 2009/10 and 2010/11, serum specimens were tested against A/California/7/2009(H1N1) and A/Perth/16/2009-like (H3N2). In 2011/12 and 2012/13 serum specimens were tested against A/California/7/2009(H1N1) and A/Victoria/361/2011-like (H3N2). Sera from consecutive years were tested in parallel due to the recommended practice of examining paired sera for evidence of influenza virus infections.

Statistical models

There were at most 13 serum specimens per participant. However, there was no H1N1 and H3N2 activity between November-December 2008 and April 2009. Therefore, serum collection in April 2009 is considered as the first round in our analysis. Post-vaccination sera are ignored in the analysis since they were only available for children who received vaccine/placebo.

We first identify influenza A epidemics during our study period based on local influenza surveillance data. We used the surveillance data to construct a proxy of incidence rate of influenza virus infections in the community, which was a good indication of incidence in the community based on hospital admissions [40]. Then, we identify relevant consecutive titers to estimate the infection risk. For each epidemic, the most recent round of serum collection prior to that epidemic is used to obtain the pre-epidemic titers, to address the non-bracketing issue [12]. Then, any titer that is collected in the next two consecutive rounds (mid-epidemic and post-epidemic titers) are used to infer infection status. Further titers are ignored due to the low sensitivity to detect infections with waning in titers over time [12]. For each epidemic, only unvaccinated participants with mid- or post-epidemic titers are included in the analysis of that epidemic, since interpretation of serology in vaccinated persons can be challenging [42].

Titers of 10, 20, 40 … 2560 are translated on a $\log_2$ scale to 1, 2, …, 9. Undetectable titers <10) are set to 0 on the same scale. While infection has traditionally been defined by 4-fold or greater rise in titers in consecutive pairs of sera, this definition is shown to be suboptimal for estimating infection risk, since some 2-fold rises may also indicate infections with smaller rises [11]. To improve this, we developed a 5-level hierarchical model to reconstruct the infection status, infection time and the unobserved HAI titer trajectory for each individual by describing the infection risk, boosting in antibody after infection and waning in antibody by integrating serology data and surveillance data (Appendix Section 2.3). Hence, we could identify infections without using a cutoff of the rise of titers to define infections in our analyses.

The first level of our model was the ‘measurement model’ (Appendix, Section 2.4). We modeled the underlying titer on a continuous scale, so that a ‘true’ titer between any two dilutions was measured as the lower of the two dilutions when there was no measurement error. For example, a “true” titer of 1.3 is measured as 1. We consider a ‘true' titer was the underlying but unmeasured titer on a continuous scale, and a ‘measured titer’ is the value that is actually measured by the assay. We use the approach in Cauchemez et al. to model the probability of 2-fold error on the left or right side [11].

The second level of the model was the HAI titer dynamics model (Appendix, Section 2.5). The magnitude of the boosting and the waning was Gamma distributed, and their characterizing parameters are

estimated in the inference. We allow these distributions to be different for children and adults, for epidemics with or without strain change compared with previous epidemic of same subtype (H1N1 or H3N2), and by subtype.

The third level of the model was the infection model (Appendix, Section 2.6), that describes the daily infection risk during epidemics. In agreement with our previous analysis [12], we assume that the scaling parameter changed on November 21, 2009 to account for the fact that the sentinel surveillance system is affected by the 2009 pandemic H1N1 outbreak [43]. The pre-epidemic titer and age groups were considered as covariates of infection risk in the model. The fourth level of the model for the distribution of pre-epidemic titer (Appendix, Section 2.7). The fifth level of the model specifies our priors on model parameters.

Model Inference

To infer the unobserved HAI titer trajectories, we use a Bayesian data augmentation framework [44]. We developed a reversible-jump Markov Chain Monte Carlo (MCMC) algorithm to explore the joint distribution of model parameters and augmented data (Appendix, Section 3). We updated model parameters with a Metropolis-Hastings algorithm. Infection times, individual boosting and waning parameters and true titers for each individual were jointly updated with a Metropolis-Hastings algorithm conditional on their augmented infection status. Finally, we used a reversible-jump MCMC approach to add or remove infections, informed by the pattern of HAI titers, and also the infection risk of a particular epidemic. Statistical analyses were conducted using R version 4.0.5 (R Foundation for Statistical Computing, Vienna, Austria).

Association between infection status in different epidemics

We utilize the longitudinal feature of our study to explore association between infection status in different epidemics (Appendix, Section 4). To estimate the association, we randomly select 100 augmented infection status in the inference to reconstructed datasets. For each reconstructed dataset, we conduct logistic regression for infection status for each pair of epidemics in our study. Hence, we could estimate the homosubtypic or heterosubtypic protection from previous infections, defined as one minus odds ratio, based on the subtypes of the pair of epidemics (Table S4). We further include the pre-epidemic HAI titer in the logistic regression, to determine if any identified protection could be explained by pre-epidemic HAI titer. We use a bootstrap approach to account for sampling uncertainty for the above analyses [37].

Model validation and adequacy

A simulation study is conducted to confirm that our algorithm could provide unbiased estimates of model parameters. In each simulation, a dataset is simulated with parameters equal to their posterior mean, and with a structure identical to the observed dataset, including the availability of titer measurement, infection status and age (Appendix, Section 5). We also track the sensitivity and specificity for using our proposed model and 4-fold cutoff to identify infections, and track the infection probabilities by age groups, and relative susceptibility among age groups computed by using a 4-fold cutoff. We check the model

adequacy by comparing the distribution of titer changes for each age group and each epidemic in observed data and the 1000 simulated epidemics.

Declarations

Acknowledgements

We thank Chan Kit Man, Kwok Hung Chan, Calvin Cheng, Lai-Ming Ho, Ho Yuk Ling, Nicole Huang, Lam Yiu Pong, Tom Lui, Edward Ma, Sophia Ng, Tong Hok Leung, Loretta Mak, Winnie Wai, Kevin Yau, and Jenny Yuen for research support. This study was supported by the Research Fund for the Control of Infectious Diseases of the Health, Welfare and Food Bureau of the Hong Kong SAR Government (grant CHP-CE-03), the Theme-based Research Scheme project no. T11-712/19N from the Hong Kong Government, the Health and Medical Research Fund, Food and Health Bureau, Government of the Hong Kong Special Administrative Region (grant no. 20190542), and the Laboratory of Excellence Integrative Biology of Emerging Infectious Diseases (research funding to SC), AXA Research Fund to SC. The funding bodies had no role in study design, data collection and analysis, preparation of the manuscript, or the decision to publish.

Author contributions

B.J.C., S.C. and T.K.T. designed research. B.J.C., V.J.F., J.Y.W, E.Y.S., R.A.P.M.P. and H.C.S. conducted the cohort study. T.K.T. analyzed data. T.K.T., B.J.C. and S.C. wrote the paper. D.K.M.I., G.M.L., and J.S.M.P. contributed to revision of the manuscript. B.J.C. and S.C. contributed equally to this work. All authors discussed the results and commented on the manuscript.

Potential conflicts of interest.

BJC reports honoraria from AstraZeneca, Sanofi Pasteur, GSK, Moderna and Roche. The authors report no other potential conflicts of interest.

References

1. Iuliano AD, Roguski KM, Chang HH, Muscatello DJ, Palekar R, Tempia S, et al. Estimates of global seasonal influenza-associated respiratory mortality: a modelling study. Lancet. 2018;391(10127):1285–300. doi: 10.1016/S0140-6736(17)33293-2. PubMed PMID: 29248255; PubMed Central PMCID: PMCPMC5935243.
2. Hayward AC, Fragaszy EB, Bermingham A, Wang L, Copas A, Edmunds WJ, et al. Comparative community burden and severity of seasonal and pandemic influenza: results of the Flu Watch cohort study. The Lancet Respiratory medicine. 2014;2(6):445–54. doi: 10.1016/S2213-2600(14)70034-7. PubMed PMID: 24717637.
3. Leung NH, Xu C, Ip DK, Cowling BJ. The Fraction of Influenza Virus Infections That Are Asymptomatic: A Systematic Review and Meta-analysis. Epidemiology. 2015. doi:

10.1097/EDE.0000000000000340. PubMed PMID: 26133025.

4. Cohen C, Kleynhans J, Moyes J, McMorrow ML, Treurnicht FK, Hellferscee O, et al. Asymptomatic transmission and high community burden of seasonal influenza in an urban and a rural community in South Africa, 2017-18 (PHIRST): a population cohort study. Lancet Glob Health. 2021;9(6):e863-e74. Epub 2021/05/22. doi: 10.1016/S2214-109X(21)00141-8. PubMed PMID: 34019838; PubMed Central PMCID: PMCPMC8262603.
5. Monto AS, Kioumehr F. The Tecumseh Study of Respiratory Illness. IX. Occurence of influenza in the community, 1966–1971. Am J Epidemiol. 1975;102(6):553–63. PubMed PMID: 1202957.
6. Riley S, Kwok KO, Wu KM, Ning DY, Cowling BJ, Wu JT, et al. Epidemiological characteristics of 2009 (H1N1) pandemic influenza based on paired sera from a longitudinal community cohort study. PLoS Med. 2011;8(6):e1000442. doi: 10.1371/journal.pmed.1000442. PubMed PMID: 21713000; PubMed Central PMCID: PMC3119689.
7. Wei VWI, Wong JYT, Perera R, Kwok KO, Fang VJ, Barr IG, et al. Incidence of influenza A(H3N2) virus infections in Hong Kong in a longitudinal sero-epidemiological study, 2009-2015. PloS one. 2018;13(5):e0197504. doi: 10.1371/journal.pone.0197504. PubMed PMID: 29795587; PubMed Central PMCID: PMCPMC5967746 following competing interests: BJC has received research funding from Sanofi Pasteur for a study of influenza vaccine effectiveness. BJC is a Section Editor of PLoS ONE. This does not alter the authors' adherence to all the PLOS ONE policies on sharing data and materials. The authors report no other potential conflicts of interest.
8. Quandelacy TM, Cummings DAT, Jiang CQ, Yang B, Kwok KO, Dai B, et al. Using serological measures to estimate influenza incidence in the presence of secular trends in exposure and immuno-modulation of antibody response. Influenza Other Respir Viruses. 2021;15(2):235–44. Epub 2020/10/28. doi: 10.1111/irv.12807. PubMed PMID: 33108707; PubMed Central PMCID: PMCPMC7902255.
9. Wood JM, Gaines-Das RE, Taylor J, Chakraverty P. Comparison of influenza serological techniques by international collaborative study. Vaccine. 1994;12(2):167–74. PubMed PMID: 8147099.
10. Katz JM, Hancock K, Xu X. Serologic assays for influenza surveillance, diagnosis and vaccine evaluation. Expert review of anti-infective therapy. 2011;9(6):669–83. doi: 10.1586/eri.11.51. PubMed PMID: 21692672.
11. Cauchemez S, Horby P, Fox A, Mai le Q, Thanh le T, Thai PQ, et al. Influenza infection rates, measurement errors and the interpretation of paired serology. PLoS Pathog. 2012;8(12):e1003061. doi: 10.1371/journal.ppat.1003061. PubMed PMID: 23271967; PubMed Central PMCID: PMC3521724.
12. Tsang TK, Fang VJ, Perera RA, Ip DK, Leung GM, Peiris JS, et al. Interpreting Seroepidemiologic Studies of Influenza in a Context of Nonbracketing Sera. Epidemiology. 2016;27(1):152–8. doi: 10.1097/EDE.0000000000000408. PubMed PMID: 26427725; PubMed Central PMCID: PMCPMC4825848.

13. Presanis AM, De Angelis D, New York City Swine Flu Investigation T, Hagy A, Reed C, Riley S, et al. The severity of pandemic H1N1 influenza in the United States, from April to July 2009: a Bayesian analysis. PLoS Med. 2009;6(12):e1000207. doi: 10.1371/journal.pmed.1000207. PubMed PMID: 19997612; PubMed Central PMCID: PMC2784967.
14. Kwok KO, Riley S, Perera R, Wei VWI, Wu P, Wei L, et al. Relative incidence and individual-level severity of seasonal influenza A H3N2 compared with 2009 pandemic H1N1. BMC Infect Dis. 2017;17(1):337. Epub 2017/05/13. doi: 10.1186/s12879-017-2432-7. PubMed PMID: 28494805; PubMed Central PMCID: PMCPMC5425986.
15. Tsang TK, Lau LL, Cauchemez S, Cowling BJ. Household Transmission of Influenza Virus. Trends in microbiology. 2016;24(2):123–33. doi: 10.1016/j.tim.2015.10.012. PubMed PMID: 26612500; PubMed Central PMCID: PMCPMC4733423.
16. Cowling BJ, Ng S, Ma ES, Cheng CK, Wai W, Fang VJ, et al. Protective efficacy of seasonal influenza vaccination against seasonal and pandemic influenza virus infection during 2009 in Hong Kong. Clin Infect Dis. 2010;51(12):1370–9. doi: 10.1086/657311. PubMed PMID: 21067351.
17. Cowling BJ, Ng S, Ma ES, Fang VJ, So HC, Wai W, et al. Protective efficacy against pandemic influenza of seasonal influenza vaccination in children in Hong Kong: a randomized controlled trial. Clin Infect Dis. 2012;55(5):695–702. doi: 10.1093/cid/cis518. PubMed PMID: 22670050.
18. Cowling BJ, Perera RA, Fang VJ, Chan KH, Wai W, So HC, et al. Incidence of influenza virus infections in children in Hong Kong in a 3-year randomized placebo-controlled vaccine study, 2009-2012. Clin Infect Dis. 2014;59(4):517–24. doi: 10.1093/cid/ciu356. PubMed PMID: 24825868.
19. Cauchemez S, Ferguson NM, Fox A, Mai le Q, Thanh le T, Thai PQ, et al. Determinants of influenza transmission in South East Asia: insights from a household cohort study in Vietnam. PLoS Pathog. 2014;10(8):e1004310. doi: 10.1371/journal.ppat.1004310. PubMed PMID: 25144780; PubMed Central PMCID: PMC4140851.
20. Horby P, Mai le Q, Fox A, Thai PQ, Thi Thu Yen N, Thanh le T, et al. The epidemiology of interpandemic and pandemic influenza in Vietnam, 2007-2010: the Ha Nam household cohort study I. Am J Epidemiol. 2012;175(10):1062–74. doi: 10.1093/aje/kws121. PubMed PMID: 22411862; PubMed Central PMCID: PMC3353138.
21. Van Kerkhove MD, Hirve S, Koukounari A, Mounts AW, group HNpsw. Estimating age-specific cumulative incidence for the 2009 influenza pandemic: a meta-analysis of A(H1N1)pdm09 serological studies from 19 countries. Influenza Other Respir Viruses. 2013;7(5):872–86. doi: 10.1111/irv.12074. PubMed PMID: 23331969.
22. Ranjeva S, Subramanian R, Fang VJ, Leung GM, Ip DKM, Perera R, et al. Age-specific differences in the dynamics of protective immunity to influenza. Nat Commun. 2019;10(1):1660. doi: 10.1038/s41467-019-09652-6. PubMed PMID: 30971703; PubMed Central PMCID: PMCPMC6458119.
23. Zhao X, Ning Y, Chen MI, Cook AR. Individual and Population Trajectories of Influenza Antibody Titers Over Multiple Seasons in a Tropical Country. Am J Epidemiol. 2018;187(1):135–43. doi:

10.1093/aje/kwx201. PubMed PMID: 29309522; PubMed Central PMCID: PMCPMC5860523.

24. Freeman G, Perera RA, Ngan E, Fang VJ, Cauchemez S, Ip DK, et al. Quantifying homologous and heterologous antibody titre rises after influenza virus infection. Epidemiology and infection. 2016;144(11):2306–16. doi: 10.1017/S0950268816000583. PubMed PMID: 27018720; PubMed Central PMCID: PMCPMC5530596.
25. Wu JT, Leung K, Perera RA, Chu DK, Lee CK, Hung IF, et al. Inferring influenza infection attack rate from seroprevalence data. PLoS Pathog. 2014;10(4):e1004054. doi: 10.1371/journal.ppat.1004054. PubMed PMID: 24699693; PubMed Central PMCID: PMC3974861.
26. Yang B, Lessler J, Zhu H, Jiang CQ, Read JM, Hay JA, et al. Life course exposures continually shape antibody profiles and risk of seroconversion to influenza. PLoS Pathog. 2020;16(7):e1008635. Epub 2020/07/24. doi: 10.1371/journal.ppat.1008635. PubMed PMID: 32702069; PubMed Central PMCID: PMCPMC7377380.
27. Gouma S, Kim K, Weirick ME, Gumina ME, Branche A, Topham DJ, et al. Middle-aged individuals may be in a perpetual state of H3N2 influenza virus susceptibility. Nat Commun. 2020;11(1):4566. Epub 2020/09/13. doi: 10.1038/s41467-020-18465-x. PubMed PMID: 32917903; PubMed Central PMCID: PMCPMC7486384.
28. Krammer F. The human antibody response to influenza A virus infection and vaccination. Nat Rev Immunol. 2019;19(6):383–97. Epub 2019/03/07. doi: 10.1038/s41577-019-0143-6. PubMed PMID: 30837674.
29. Hsu JP, Zhao X, Chen MI, Cook AR, Lee V, Lim WY, et al. Rate of decline of antibody titers to pandemic influenza A (H1N1-2009) by hemagglutination inhibition and virus microneutralization assays in a cohort of seroconverting adults in Singapore. BMC Infect Dis. 2014;14:414. doi: 10.1186/1471-2334-14-414. PubMed PMID: 25066592; PubMed Central PMCID: PMC4133624.
30. Ng S, Fang VJ, Ip DK, Chan KH, Leung GM, Peiris JS, et al. Estimation of the association between antibody titers and protection against confirmed influenza virus infection in children. J Infect Dis. 2013;208(8):1320–4. doi: 10.1093/infdis/jit372. PubMed PMID: 23908481; PubMed Central PMCID: PMC3778972.
31. Hoa LNM, Sullivan SG, Mai LQ, Khvorov A, Phuong HVM, Hang NLK, et al. Influenza A(H1N1)pdm09 but not A(H3N2) virus infection induces durable sero-protection: results from the Ha Nam Cohort. J Infect Dis. 2020. Epub 2020/06/03. doi: 10.1093/infdis/jiaa293. PubMed PMID: 32484513.
32. Stephenson I, Das RG, Wood JM, Katz JM. Comparison of neutralising antibody assays for detection of antibody to influenza A/H3N2 viruses: an international collaborative study. Vaccine. 2007;25(20):4056–63. Epub 2007/04/07. doi: 10.1016/j.vaccine.2007.02.039. PubMed PMID: 17412461.
33. Tsang TK, Cauchemez S, Perera RA, Freeman G, Fang VJ, Ip DK, et al. Association between antibody titers and protection against influenza virus infection within households. J Infect Dis. 2014;210(5):684–92. doi: 10.1093/infdis/jiu186. PubMed PMID: 24676208; PubMed Central PMCID: PMC4148604.

34. Ng S, Nachbagauer R, Balmaseda A, Stadlbauer D, Ojeda S, Patel M, et al. Novel correlates of protection against pandemic H1N1 influenza A virus infection. Nat Med. 2019;25(6):962–7. Epub 2019/06/05. doi: 10.1038/s41591-019-0463-x. PubMed PMID: 31160818; PubMed Central PMCID: PMCPMC6608747.
35. Coudeville L, Bailleux F, Riche B, Megas F, Andre P, Ecochard R. Relationship between haemagglutination-inhibiting antibody titres and clinical protection against influenza: development and application of a bayesian random-effects model. BMC Med Res Methodol. 2010;10:18. doi: 10.1186/1471-2288-10-18. PubMed PMID: 20210985; PubMed Central PMCID: PMC2851702.
36. Mossong J, Hens N, Jit M, Beutels P, Auranen K, Mikolajczyk R, et al. Social contacts and mixing patterns relevant to the spread of infectious diseases. PLoS Med. 2008;5(3):e74. doi: 10.1371/journal.pmed.0050074. PubMed PMID: 18366252; PubMed Central PMCID: PMC2270306.
37. Salje H, Cummings DAT, Rodriguez-Barraquer I, Katzelnick LC, Lessler J, Klungthong C, et al. Reconstruction of antibody dynamics and infection histories to evaluate dengue risk. Nature. 2018;557(7707):719–23. doi: 10.1038/s41586-018-0157-4. PubMed PMID: 29795354; PubMed Central PMCID: PMCPMC6064976.
38. Wu JT, Cowling BJ, Lau EH, Ip DK, Ho LM, Tsang T, et al. School closure and mitigation of pandemic (H1N1) 2009, Hong Kong. Emerg Infect Dis. 2010;16(3):538–41. doi: 10.3201/eid1603.091216. PubMed PMID: 20202441; PubMed Central PMCID: PMC3206396.
39. Chen MI, Cook AR, Lim WY, Lin R, Cui L, Barr IG, et al. Factors influencing infection by pandemic influenza A(H1N1)pdm09 over three epidemic waves in Singapore. Influenza Other Respir Viruses. 2013;7(6):1380–9. doi: 10.1111/irv.12129. PubMed PMID: 23829633.
40. Wong JY, Wu P, Nishiura H, Goldstein E, Lau EH, Yang L, et al. Infection fatality risk of the pandemic A(H1N1)2009 virus in Hong Kong. Am J Epidemiol. 2013;177(8):834–40. doi: 10.1093/aje/kws314. PubMed PMID: 23459950; PubMed Central PMCID: PMC3658096.
41. Cowling BJ, Chan KH, Fang VJ, Lau LL, So HC, Fung RO, et al. Comparative epidemiology of pandemic and seasonal influenza A in households. N Engl J Med. 2010;362(23):2175–84. doi: 10.1056/NEJMoa0911530. PubMed PMID: 20558368; PubMed Central PMCID: PMC4070281.
42. Petrie JG, Ohmit SE, Johnson E, Cross RT, Monto AS. Efficacy studies of influenza vaccines: effect of end points used and characteristics of vaccine failures. J Infect Dis. 2011;203(9):1309–15. doi: 10.1093/infdis/jir015. PubMed PMID: 21378375; PubMed Central PMCID: PMC3069734.
43. Marmara V, Cook A, Kleczkowski A. Estimation of force of infection based on different epidemiological proxies: 2009/2010 Influenza epidemic in Malta. Epidemics. 2014;9C:52–61. doi: 10.1016/j.epidem.2014.09.010. PubMed PMID: 25480134.
44. Gilks WR, Richardson S, Spiegelhalter D. Markov Chain Monte Carlo in Practice. London: Chapman & Hall; 1996.

Figures

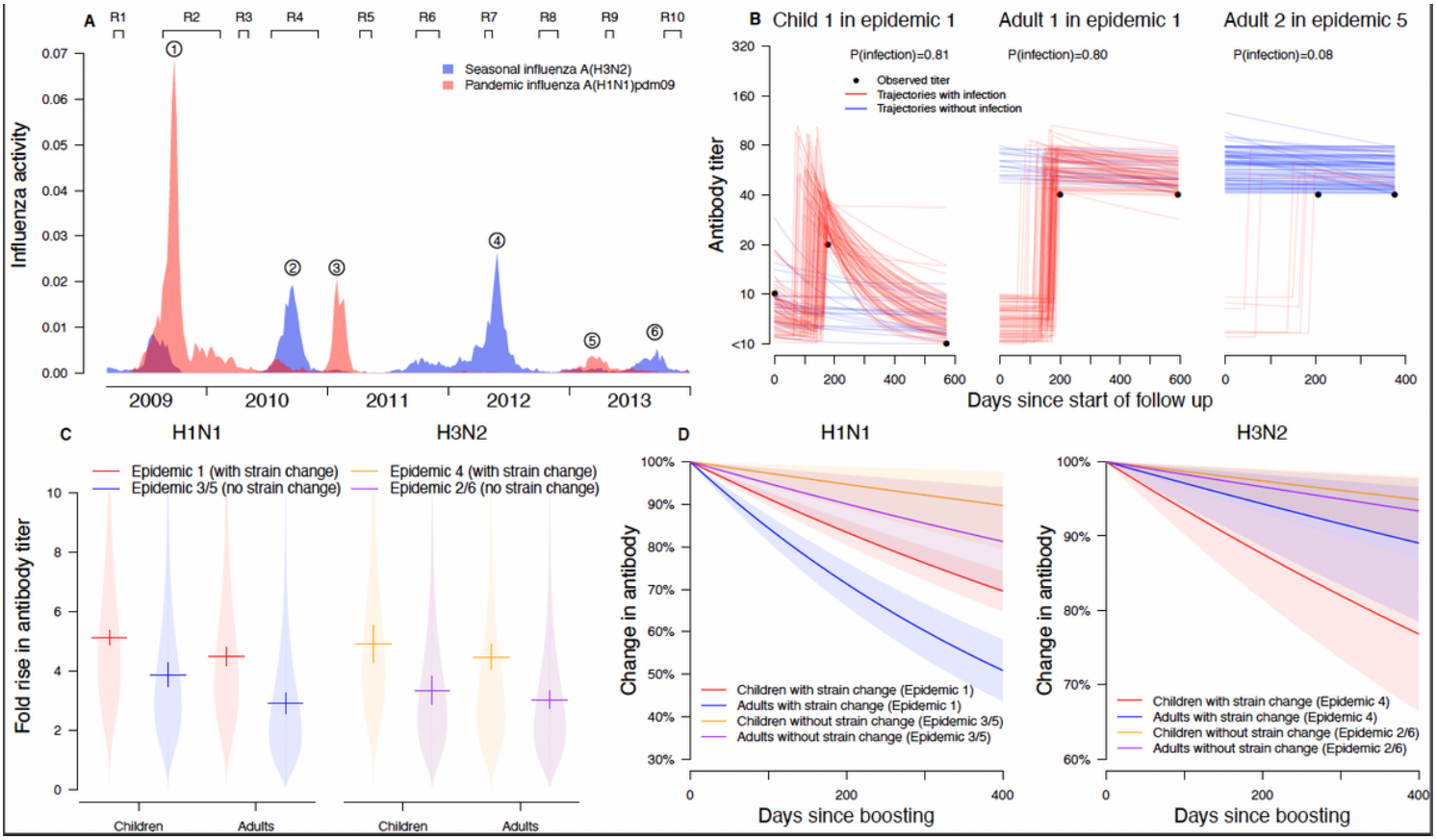

Figure 1

Estimation of individual HAI titer trajectories. Panel A. Timelines of our study, rounds of blood sample collection, and local influenza activity by surveillance data. Panel B: Illustration of HAI titer trajectories, infection status, infection time and pre-epidemic HAI titer if missing in three example individuals. The black dot represents the observed HAI titer, the curve indicates the augmented HAI titer trajectories since the start of an epidemic, red and blue indicate infection and non-infection respectively. Child 1 with 2-fold rise is imputed to be infected in some augmented data to reflect the uncertainty. Adult 1 and 2 with missing pre-epidemic HAI titer, the mid- and post-epidemic HAI titer 3 in log2 scale, are from epidemic 1 and 5 respectively. Adult 1 and 2 is estimated to be infected with probability 0.80 and 0.08 respectively. It is because 1) the pre-epidemic titer distribution suggested that adult 3 has a higher pre-epidemic titer than adult 2 (probability of <10 was 0.98 and 0.59 in epidemic 1 and 5 respectively), 2) the infection probability for adults for epidemic 1 (18%) was higher than epidemic 5 (2%). Panel C: Estimated boosting distribution in HAI titer after infection by subtype. Funnel plots are used to show the distribution and solid lines are used to show the mean and corresponding 95% credible intervals. Panel D. The waning after boosting in HAI titer from infection by subtype. The solid lines are used to show the mean waning of HAI titer trajectories over time and the shadowed areas are used to show the corresponding 95% credible intervals.

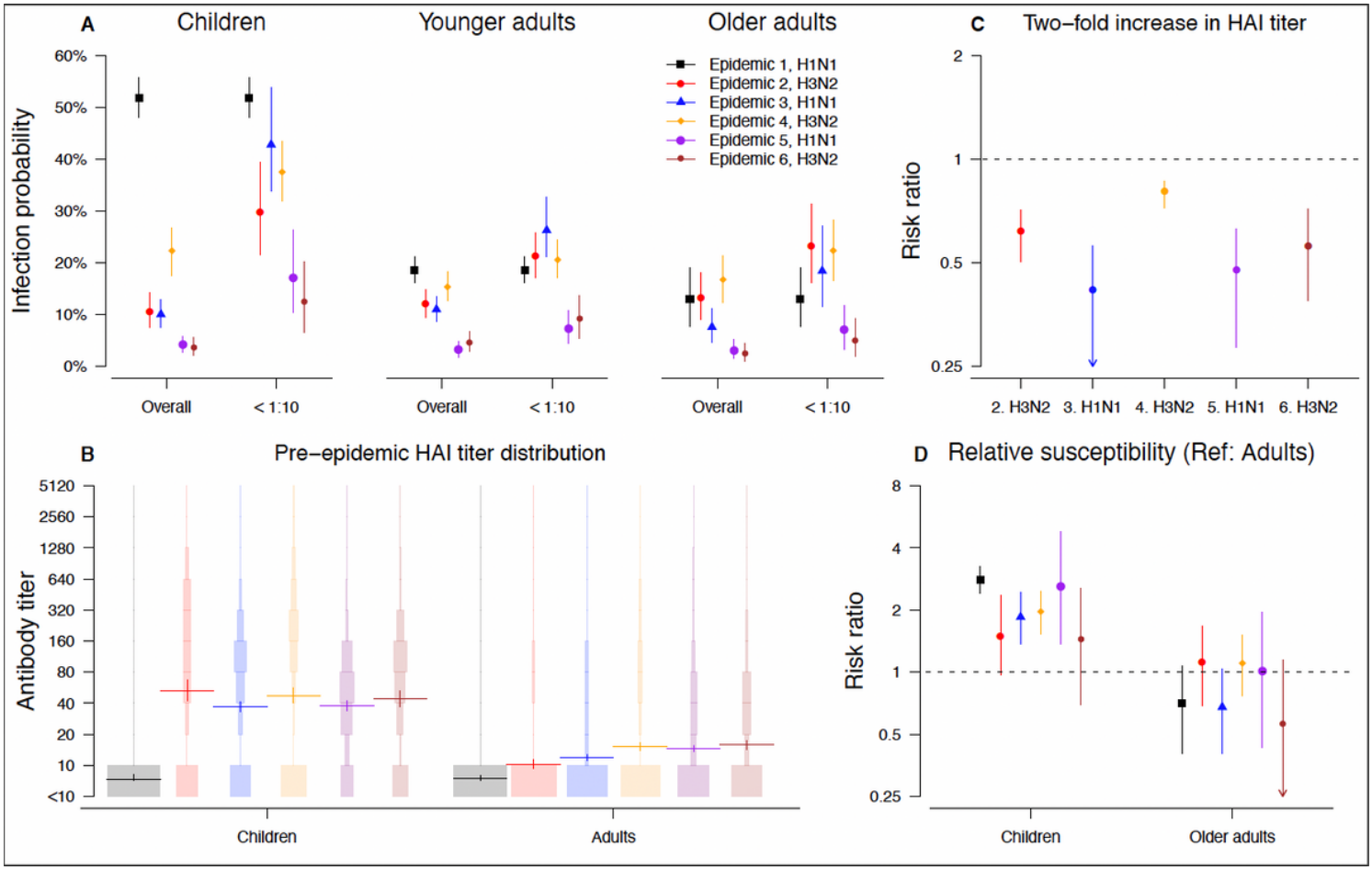

Figure 2

Infection probability and its determinant among six epidemics. Panel A. Estimates of infection probabilities for children, younger adults and older adults in the six epidemics in our study period. The overall infection probability and infection probability for individuals with pre-epidemic titer of <10 are plotted to show the protective effect of pre-epidemic titers. Panel B. The protection associated with 2-fold increase in HAI titers in epidemic 2-6. Panel C. The pre-epidemic HAI titer distribution for children and adults in the six epidemics. Funnel plots are used to show the distribution and solid lines are used to show the mean and corresponding 95% credible intervals. Panel D. Model estimate of the age-relative susceptibility for six epidemics.

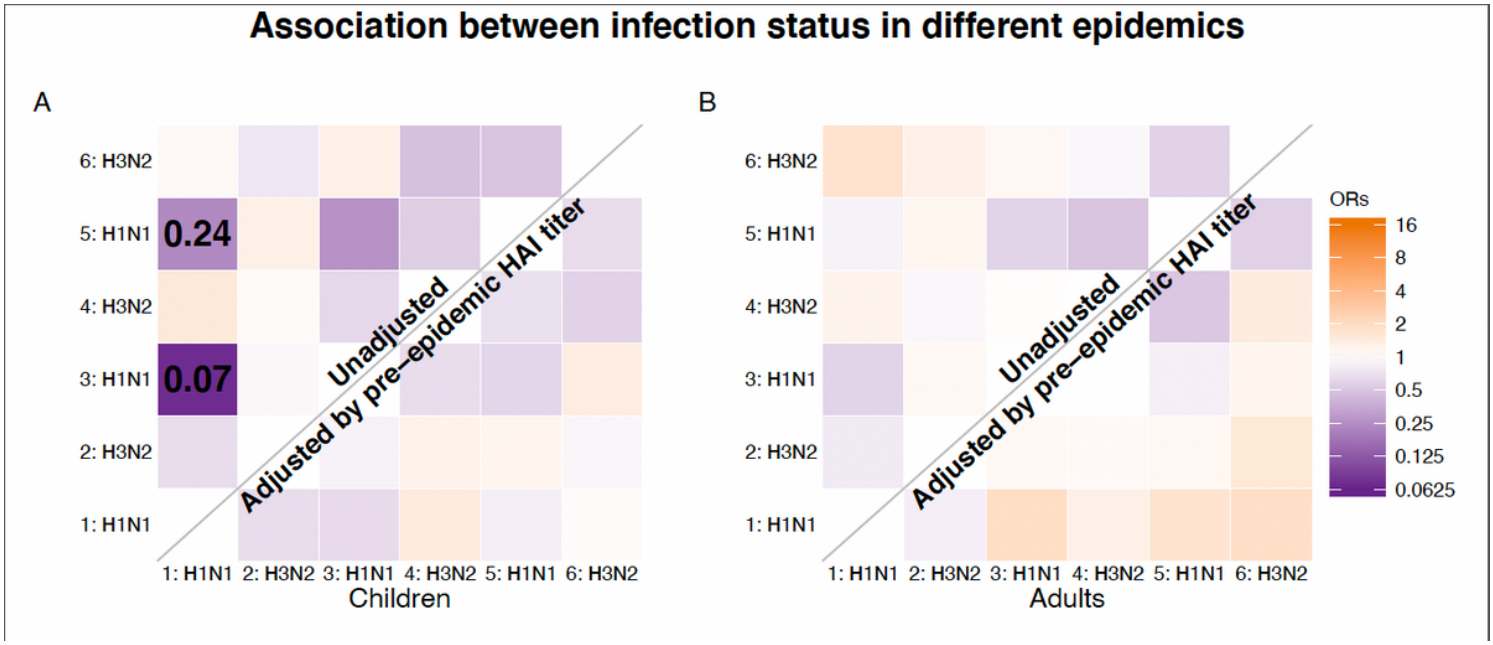

Figure 3

The association between infection status in different epidemics. The association between the infection status in each pair of epidemics in the study period. Upper and lower diagonal shows the odds ratio without adjustment and adjusting pre-epidemic HAI titer respectively. Panel A and B indicate the association for children and adults respectively.

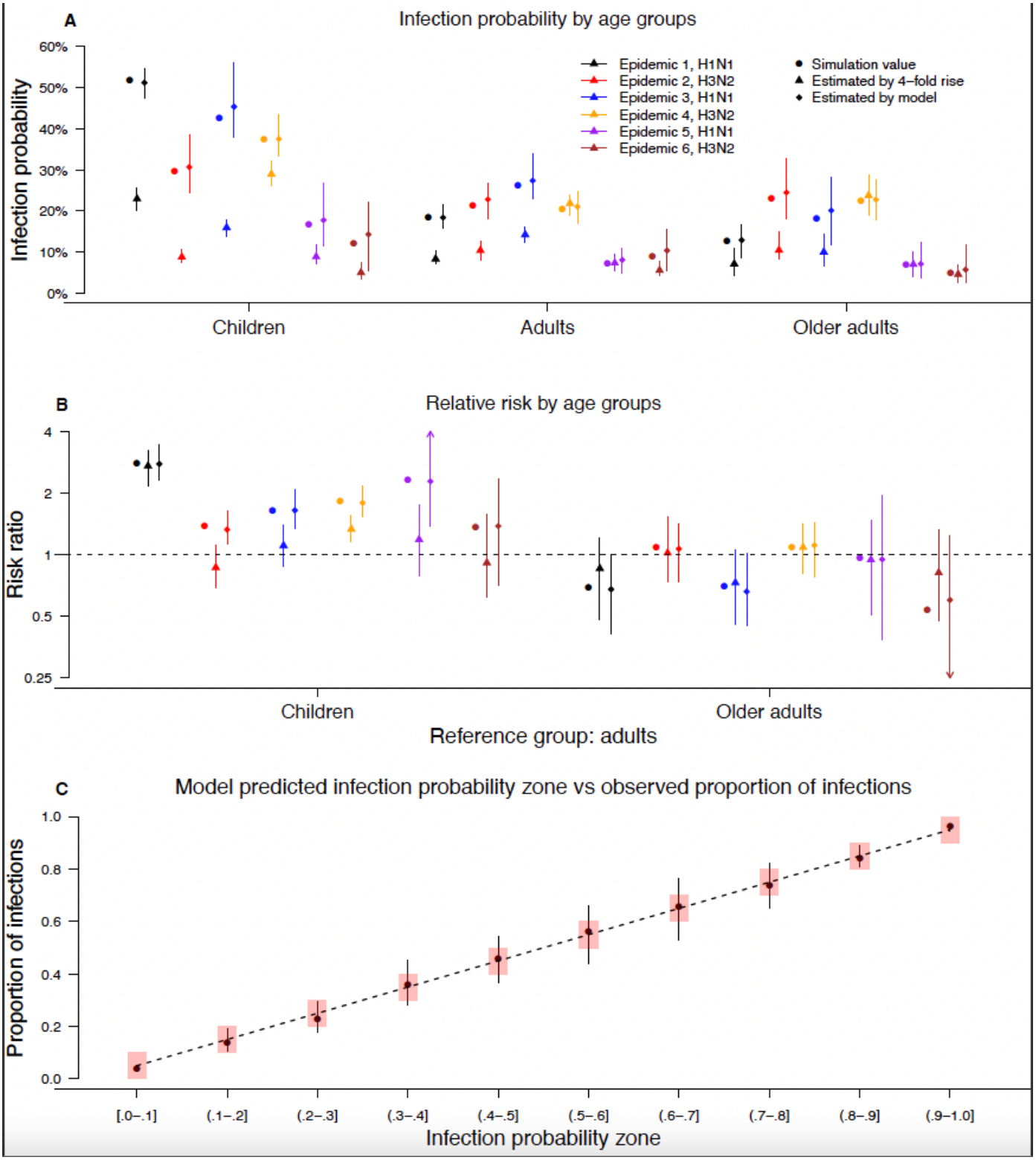

Figure 4

Comparison of using 4-fold cutoff and using model estimates to estimate infection probabilities and relative susceptibility among age groups by simulation. Panel A and B show the infection probabilities and relative susceptibility among age groups estimated by a 4-fold cutoff and by our proposed approach respectively. Panel C. The proportion of infected individuals in the groups with different infection probability zone (red rectangles) estimated by our inference from simulation study.

Supplementary Files

This is a list of supplementary files associated with this preprint. Click to download.

- infectionriskSI20oct.docx
- figureS1.pdf
- figureS2.pdf
- figureS3.pdf